CELLO MEASUREMENTS FOR LOCAL AND GLOBAL CHARACTERIZATION OF GRID FINGER, CONTACT, AND EMITTER RESISTANCE LOSSES OF LARGE AREA SOLAR CELLS

J. Carstensen, A. Schütt, A. Pape, and H. Föll
Chair for General Materials Science, Faculty of Engineering, Christian-Albrechts-University of Kiel,
Kaiserstr. 2, 24143 Kiel, Germany, email: jc@tf.uni-kiel.de, Phone: (+49) 431 880 6181, Fax: (+49) 431 880 6178

ABSTRACT: CELLO voltage measurements allow already for a fully quantitative analysis of local ohmic losses but the reasons for the ohmic losses could only be estimated from the shape of the loss structure. A better understanding especially of the frequency dependency of the current transport through pn-junction, emitter, contact resistance, and grid finger allows now for a direct correlation to these ohmic loss mechanisms. It is demonstrated on a large multicrystalline Si solar cell with inhomogeneous sheet resistance of the emitter, to identify the reasons of different serial resistance losses, e.g. distinguishing areas with high contact resistances or high sheet resistances. Further, an impedance measurement and the fit to the standard 1D model is introduced to extract global serial resistance and diode resistance.

Keywords: characterization, series resistance, contact,

1 INTRODUCTION

Especially on large area solar cells with high efficiencies small ohmic losses are decisive. New contacting concepts like selective emitter reflect this importance, but of course analytical tools which allow for the measurements of local resistances with a high spatial resolution are essential for further improvements. CELLO voltage measurements allow already for a fully quantitative analysis of local ohmic losses but the reasons for the ohmic losses could only be estimated from the shape of the loss structure. A better understanding especially of the frequency dependency of the current transport through pn-junction, emitter, contact resistance, and grid finger allows now for a direct correlation to the above mentioned ohmic loss mechanisms.

2 MODELLING OF SERIAL RESISTANCES

For a quantitative calculation of local serial resistances from local voltage maps it is sufficient to use a quite simple analytical description of a 2D network of a solar cell [1]

$$R(x) = \frac{U(x)}{dI_0} = \frac{\rho}{2\pi\sqrt{\frac{\rho KA}{\pi}}} \frac{I_0\left(\sqrt{\frac{\rho KAx}{\pi}}\right)}{I_1\left(\sqrt{\frac{\rho KA}{\pi}}\right)}, \qquad (1)$$

here I_0 and I_1 are the modified Bessel functions of 0. and 1. kind, ρ is an effective sheet resistance, x is a fraction number between 0 and 1.0 for the area of the solar cell. Choosing

$$KA = \frac{1}{R_D} + i\omega C \qquad (2).$$

even the frequency dependence for intensity modulated current flow through a solar cell can be calculated. Here R_D is the global diode resistance and C the global capacitance of the pn-junction. Eq. (1) correlates the specific parameters of a 2D network with the resistances of the standard 1D equivalent circuit as shown in Fig. 1a). In particular it predicts a linear relation for the voltage distribution across any 2D network of a solar cell which has been found for nearly all solar cells ever investigated with the CELLO system and which allows to quantify serial resistances [1]. An example for a measured linear distribution as well as a fit to the straight line is shown in Fig. 1b) for the solar results cell shown in Fig. 2. One important consequence of Eq. (1) is that the 2D network can only be represented by a 1D equivalent circuit if $R_D > R_{ser}$. Since the capacitance is parallel to R_D, a second condition for the applicability of a 1D model is $1 / | i \omega C | > R_{ser}$, i.e. only for small frequencies a 2D network of a solar cell can be described by the frequency dependence of the 1D equivalent circuit of Fig. 1a) which mainly is given by a resistor and capacitor connected in parallel

$$\frac{1}{1+i\omega RC}, \ (3) \qquad \varphi(\omega) \approx \tan\varphi = \omega RC\,(+const.) \ .(4)$$

Thus in any measurement of a 1D network a phase shift proportional to the applied frequency will be found. The additional *const.* refers to additional phase shifts, e.g. from minority diffusion when generating local currents by a Laser beam. Therefore for two phase shifts of e.g. local photo induced voltages measured at different frequencies the pure 1D frequency dependency can be separated from 2D frequency dependencies by the procedures

$$\varphi(\omega_1) - \varphi(\omega_2), \ (5) \qquad \frac{\varphi(\omega_1)}{\omega_1} - \frac{\varphi(\omega_2)}{\omega_2}, \quad (6)$$

The procedure of Eq. (5) will eliminate phase shifts with a weak frequency dependency, the procedure of Eq. (6) will eliminate all phase shifts showing a linear frequency dependency. CELLO maps are generated by measuring the current or voltage response of locally Laser induced charges. For this current the flow through one of the grid fingers is a 1D transport although all grid fingers together form a 2D network. The same is true for the contact resistance losses, while the current transport through the emitter even for local illumination is intrinsically a current transport through a 2D structure. The above discussed corresponding frequency dependencies will help to distinguish the different ohmic loss mechanisms.

3 EXPERIMENTAL RESULTS AND DISCUSSION

Fig. 2 shows CELLO results of open circuit voltage maps measured with two different frequencies of a multicrystalline solar cell showing several areas with resistance losses related to chemical etching of the emitter. The measurements have been performed at 1/3 sun illumination using a 934 nm LASER with a focus size of 400 µm. The serial resistance map in Fig. 2b) has been calculated combining the open circuit voltage map in Fig. 2a), the short circuit current map in Fig. 3a) and the fit of the global iv-curve as described in detail in [1]. As mentioned before Eq. (1) implies, that the fit of the global iv-curve to the standard iv-curve model may lead to errors in strong forward direction. An alternative to get more correct numbers for the global serial resistance, the global diode resistance, and the capacitance of the solar cell are frequency dependent voltage impedance measurements which can be performed at any point along the iv-curve and which can be fitted to the equivalent circuit in Fig. 1a) as well. Fig. 1c) shows as an example the Nyquist plots of the impedance of the solar cell discussed in Fig. 2. From these data the diode resistance of the solar cell was fitted a shown in Fig. 1d) for several voltages in forward direction. Since this paper focuses on the local characterization we will not discuss further the pro's and con's of such an approach. It is just important to note that by taking into account the values of the global serial resistance the numbers presented for the serial resistance in Fig. 3b) are correct, i.e. they reflect the resistance loss from the illuminated spot to the main bus bars where the current is extracted from the solar cell. Although Fig. 3b) quantifies all local series resistances, it does not directly allow for identification of the resistance type. The identification is possible from the phase shift maps Fig. 2b) and Fig. 2d) and an interpretation following the Eqs. (4) - (6). Fig. 3c) shows the difference of the phase shifts of Fig. 2b) and Fig. 2d) according to Eq. (5). Fig. 3d) shows the frequency corrected difference of the phase shifts of Fig. 2b) and Fig. 2d) according to Eq. (6). Several areas are marked in the serial resistance map in Fig. 3b). To allow for a more efficient discussion of the maps the result will be summarized in advance: region A shows broken grid fingers; region B are contact problems between emitter and grid finger due to a strong chemical thinning of the emitter; region C contains lines where drops thinned the emitter, which has no impact on the contact resistance but just increases the lateral emitter resistance; region D has a nearly infinite contact resistance between emitter and grid (due to an extreme chemical thinning of the emitter), current transport is only possible taking long paths through the emitter; region E does not have a bad ohmic contact to the solar cell, but in forward direction a lateral current flow into this regions (to compensate for the differences in short circuit current) induces the ohmic losses visible in this area. Most of the features mentioned above become plausible just taking into account the shape of the areas with increased serial resistance, only the distinction of the regions B, C and D really need the maps in Fig. 3c) and Fig. 3d). Region B is a dark area in Fig. 3c) but not in Fig. 3d). This is a clear hint, that these ohmic losses are related to contact problems, but no relevant losses are related to a 2D current flow, i.e. losses in the emitter. Region D is a completely dark region in Fig. 3d) but only parts of that region are dark in Fig. 3c). Of course this way of discussion is difficult; the power of this analysis only become clear when applying it to various types of solar cells with various types of resistance problems. A more simple example is shown in Fig. 4 of a monocrystalline solar cell. All structures visible in the resistance map in Fig. 4a) show up "inverted" in Fig. 4b). Nearly non of this features are visible in Fig. 4c).

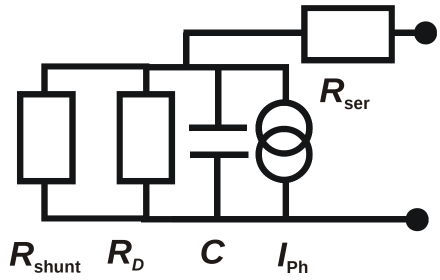

a)

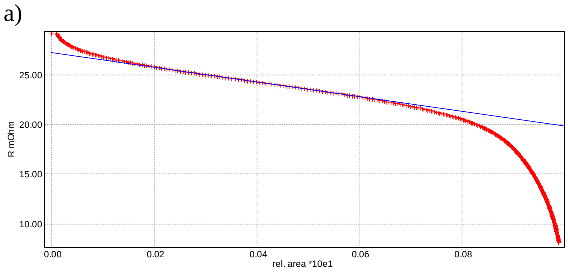

b)

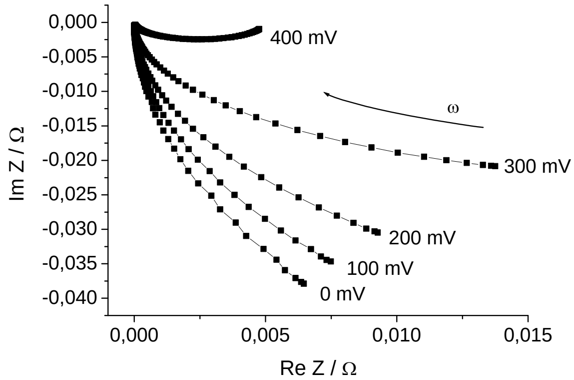

c)

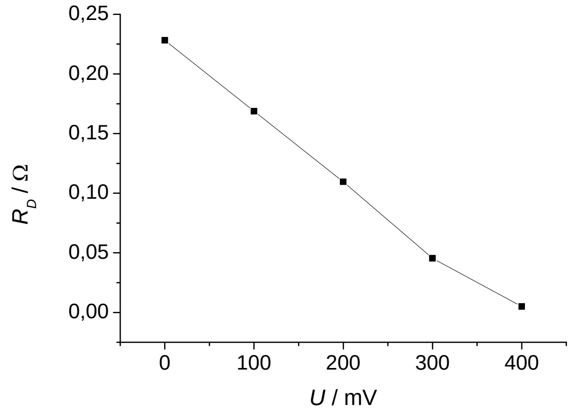

d)

Figure 1: a) Standard equivalent circuit of a solar cell; b) Resistance distribution extracted from histogram of Fig. 2a); c) solar cell impedance for several points along iv-curve; d) diode resistance from fitting impedance curves in c).

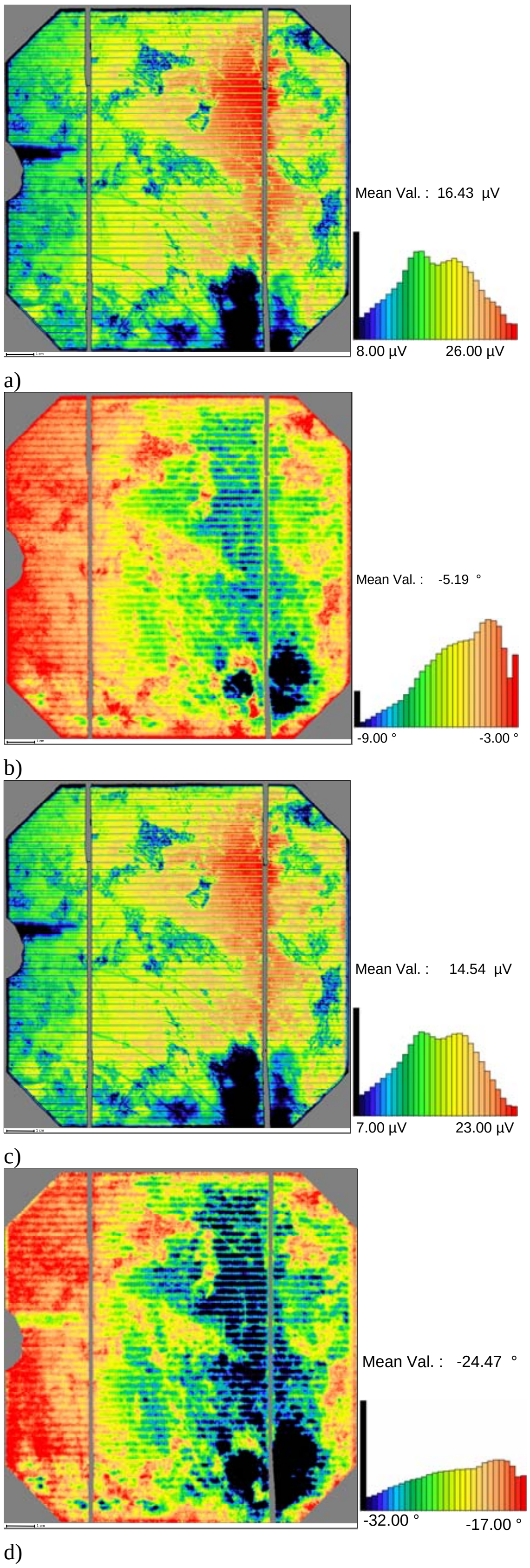

Figure 2: Open circuit voltage dU_{OC} measurements of different modulation frequencies on a mc-Si solar cell with emitter problems (details text): Amplitude (a) and phase shift (b) map for 4518 Hz; and amplitude (c) and phase shift (d) map for 19736 Hz.

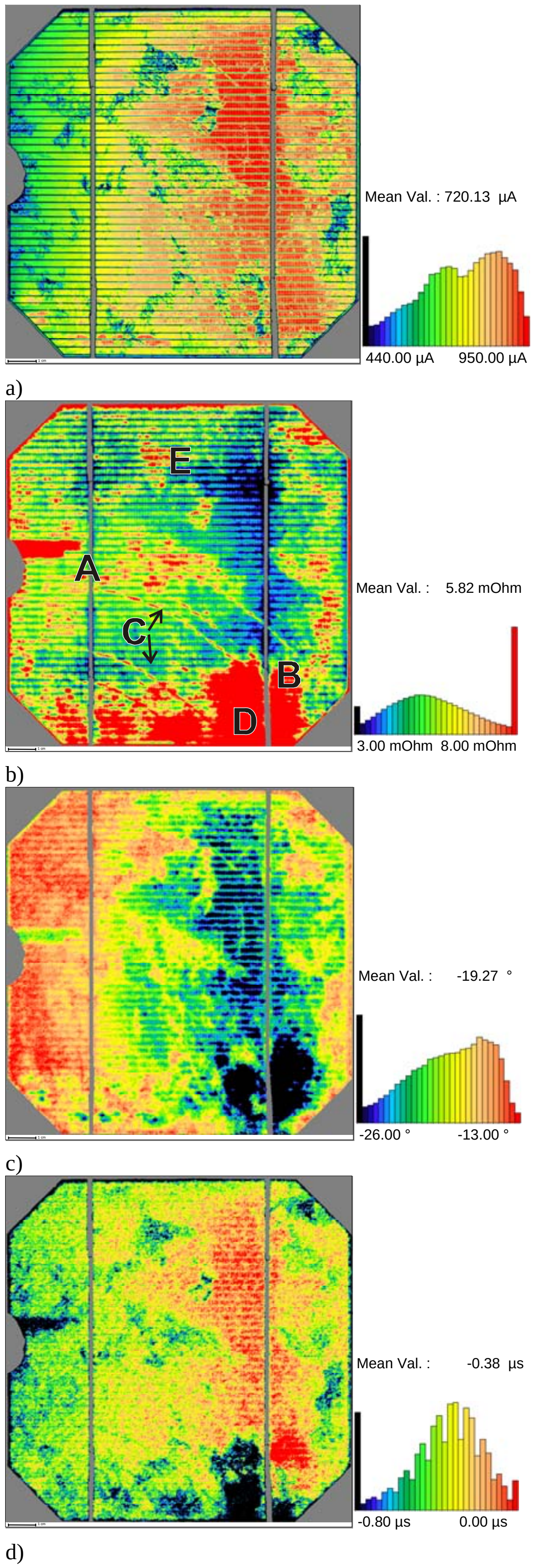

Figure 3: a) dI_{SC} measurement; b) Standard CELLO serial resistance map extracted from Fig. 1a), Fig. 2a), and Fig. 3a); c) Phase shift difference according to Eq. (5) of Fig. 1b) and Fig. 1d); d) Phase shift difference according to Eq. (6) of Fig. 1b) and Fig. 1d).

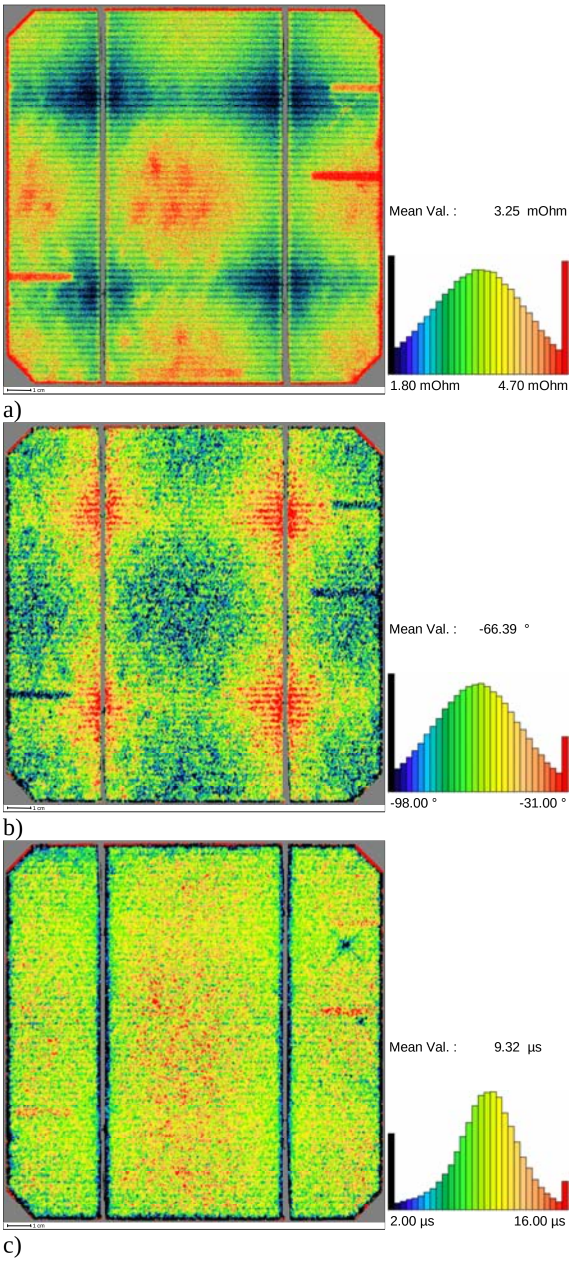

Figure 4: Maps of a mono Si with injection level dependent photo current: a) Standard CELLO serial resistance map (cf. Fig. 2a); b) Phase shift difference according to Eq. (5), cf. Fig. 2c); and c) Phase shift difference according to Eq. (6), cf. Fig. 2d).

In Fig. 4c) in the right upper part only one dark spot is visible from which 4 lines under 90° are starting. This is the typical structure of a crack cutting through the emitter as well. But obviously the grid fingers are not destroyed. The cross like structure is slightly visible in the serial resistance map Fig. 4a) as well but not in Fig. 4b). A crack through an emitter leads to larger ohmic losses for the 2D current transport through the emitter. No change in the contact resistance, i. e. a 1D loss mechanism, is expected. So this example is again in perfect agreement with the model outlined here for the interpretation of the frequency dependent phase shift behavior of different types of ohmic losses. The only drawback of this approach of analyzing the frequency dependent phase shift response is the necessity of measuring the solar cell twice for two frequencies. As routinely done for short circuit current measurements [2] the two frequencies could be applied to the Laser intensity simultaneously and analyzed by FFT deconvolution simultaneously scanning just once the solar cell. Since signal to noise ration is a more severe problem for voltage measurements than for current measurements, this has not been implemented up to now. Strategies using two signals with very different amplitudes may help to overcome this problem in near future.

4 SUMMARY

Serial resistance losses on all commercially available solar cells and a large number of lab solar cells can be quantitatively analyzed using the CELLO technique.

Various types of resistance losses like broken grid fingers, contact losses, emitter problems can be distinguished analyzing the frequency dependent phase shift of the open circuit voltage measurements.

In the near future measurement time for this type of analysis will be drastically reduced by simultaneous measurements at several frequencies as already implemented for short circuit measurements.

5 ACKNOWLEDGMENTS

We like to thank the Fraunhofer ISE in Gelsenkirchen for the supply of solar cells with various firing conditions.

6 REFERENCES

[1] J. Carstensen, A. Abdollahinia, A. Schütt, and H. Föll, in Proceedings of the 24th European Photovoltaic Solar Energy Conference, 1CV.4.33, Hamburg (2009).

[2] J. Carstensen, A. Schütt, and H. Föll, in Proceedings of the 24th European Photovoltaic Solar Energy Conference, 1AO.4.5, Hamburg (2009).